Integrating Multisector Molecular Characterization into Personalized Peptide Vaccine Design for Patients with Newly Diagnosed Glioblastoma

Tanner M. Johanns[1,2,3], Elizabeth A.R. Garfinkle[4], Katherine E. Miller[4], Alexandra J. Livingstone[1], Kaleigh F. Roberts[5], Lakshmi P. Rao Venkata[4], Joshua L. Dowling[3,6], Michael R. Chicoine[7], Ralph G. Dacey[6], Gregory J. Zipfel[3,6], Albert H. Kim[3,6], Elaine R. Mardis[4,8], and Gavin P. Dunn[9,10]

ABSTRACT

Purpose: Outcomes for patients with glioblastoma (GBM) remain poor despite multimodality treatment with surgery, radiation, and chemotherapy. There are few immunotherapy options due to the lack of tumor immunogenicity. Several clinical trials have reported promising results with cancer vaccines. To date, studies have used data from a single tumor site to identify targetable antigens, but this approach limits the antigen pool and is antithetical to the heterogeneity of GBM. We have implemented multisector sequencing to increase the pool of neoantigens across the GBM genomic landscape that can be incorporated into personalized peptide vaccines called NeoVax.

Patients and Methods: In this study, we report the findings of four patients enrolled onto the NeoVax clinical trial (NCT0342209).

Results: Immune reactivity to NeoVax neoantigens was assessed in peripheral blood mononuclear cells pre- and post-NeoVax for patients 1 to 3 using IFNγ-ELISPOT assay. A statistically significant increase in IFNγ producing T cells at the post-NeoVax time point for several neoantigens was observed. Furthermore, a post-NeoVax tumor biopsy was obtained from patient 3 and, upon evaluation, revealed evidence of infiltrating, clonally expanded T cells.

Conclusions: Collectively, our findings suggest that NeoVax stimulated the expansion of neoantigen-specific effector T cells and provide encouraging results to aid in the development of future neoantigen vaccine–based clinical trials in patients with GBM. Herein, we demonstrate the feasibility of incorporating multisector sampling in cancer vaccine design and provide information on the clinical applicability of clonality, distribution, and immunogenicity of the neoantigen landscape in patients with GBM.

Introduction

Glioblastoma (GBM) is the most common malignant central nervous system tumor in adults. The current treatment paradigm involves maximum safe surgical resection and radiotherapy concurrently with temozolomide chemotherapy followed by adjuvant maintenance temozolomide (1). Despite this aggressive multimodality approach, GBM remains lethal and inevitably recurs, at which point there are limited effective options. Although the median survival for patients diagnosed with GBM remains a dismal 15 to 20 months, it has become clear that the methylation status of the O^6-methylguanine methyltransferase (MGMT) gene promoter within a patient's tumor represents an important biomarker of response to temozolomide (2). Specifically, the majority of patients whose tumors carry an unmethylated MGMT gene promoter do not respond to temozolomide (3). This lack of response has led to clinical trials exploring novel treatments for patients with newly diagnosed unmethylated MGMT GBM to omit temozolomide chemotherapy due to its lack of efficacy and to mitigate associated toxicities. Thus, there is an urgent need for improved therapeutic strategies for GBM, specifically for patients of the MGMT unmethylated subgroup, as only surgery and radiation have demonstrated any impact on outcomes (4–6).

Because immune checkpoint inhibitor (ICI) therapy has revolutionized the treatment of a range of malignancies in the last several years, there has been tremendous enthusiasm to examine the effectiveness of ICI treatment in patients with brain tumors as well. However, phase 3 studies did not show a clinical benefit of PD1 blockade ICI monotherapy for patients with GBM (4, 5), and thus there remain no FDA-approved immunotherapies for primary GBM. Several reasons may underlie this observation, including modest mutational burden, a relative paucity of tumor-infiltrating lymphocytes, intratumoral neoantigen heterogeneity, and other glioma immunoediting networks (7). Nevertheless, several studies have suggested that personalized neoantigen vaccines may lead to

[1]Division of Medical Oncology, Washington University School of Medicine, St. Louis, Missouri. [2]Andrew M. and Jane M. Bursky Center for Human Immunology and Immunotherapy Programs, Washington University School of Medicine, St. Louis, Missouri. [3]The Brain Tumor Center at Siteman Cancer Center, Washington University School of Medicine, St. Louis, Missouri. [4]The Steve and Cindy Rasmussen Institute for Genomic Medicine, Nationwide Children's Hospital, Columbus, Ohio. [5]Department of Pathology and Immunology, Washington University School of Medicine, St. Louis, Missouri. [6]Department of Neurological Surgery, Washington University School of Medicine, St. Louis, Missouri. [7]Department of Neurosurgery, University of Missouri in Columbia, Columbia, Missouri. [8]Department of Pediatrics, Ohio State University College of Medicine, Columbus, Ohio. [9]Department of Neurosurgery, Harvard Medical School, Massachusetts General Hospital, Boston, Massachusetts. [10]Brain Tumor Immunology and Immunotherapy Program, Department of Neurosurgery, Harvard Medical School, Massachusetts General Hospital, Boston, Massachusetts.

T.M. Johanns and E.A.R. Garfinkle contributed equally to this article.

Corresponding Author: Gavin P. Dunn, Massachusetts General Hospital, White 502, 55 Fruit Street, Boston, MA 02114. E-mail: gpdunn@mgh.harvard.edu

Clin Cancer Res 2024;30:2729–42

doi: 10.1158/1078-0432.CCR-23-3077

Translational Relevance

In this study, we illustrate the use of multi-region sequencing and corresponding analytics to generate synthetic long peptide vaccines for the treatment of patients with primary glioblastoma. Our work provides insight into the tumor immune microenvironment and demonstrates preliminary evidence that personalized peptide neoantigen vaccines can stimulate a clonal expansion of tumor-directed effector T cells. Our collective findings will guide the development of next-generation neoantigen vaccine–based clinical trials for patients with glioblastoma, a group for which the current standard of care is ineffective and immunotherapy options are limited. Our results also lay the groundwork for future combinatorial studies that may include personalized neoantigen vaccines with standard-of-care radiotherapy and chemotherapy, or with checkpoint inhibitors to modulate immunosuppressive tumor microenvironments either concurrent with or subsequent to cancer vaccine administration.

improved responses when combined with PD1 blockade in several solid tumors (8, 9). Therefore, it is possible that strategies to augment ICI therapy, rather than employing ICI as monotherapy, may lead to better outcomes and provides a strong rationale to evaluate the use of a personalized neoantigen vaccine with ICI in GBM.

We and others have shown that a personalized neoantigen vaccine approach is feasible in GBM and can effectively elicit patient tumor-specific T-cell responses capable of infiltrating the brain microenvironment, despite the fact GBM tumors typically carry few immunogenic variants and have immunosuppressive tumor microenvironments (10–12). Specifically, we previously reported treatment of a GBM subject with a personalized peptide vaccine after autologous tumor lysate dendritic cell vaccination and identified the presence of lymphocytes from the peripheral blood and tumor microenvironment that were reactive to several HLA class I and class II candidate neoantigens (11). Keskin and colleagues conducted a phase Ib study in which personalized neoantigen vaccines were developed for subjects with newly diagnosed MGMT methylated GBM and reported an increase in tumor-infiltrating T cells that migrated from the peripheral blood after vaccination (10). In addition, Hilf and colleagues reported a phase 1 study in which patients with GBM were treated first with a vaccine composed of unmutated GBM–associated epitopes from a pre-manufactured library, followed by a second vaccine composed of personalized neoantigens based on the transcriptomes and immunopeptidomes of each individual tumor. They reported that the initial unmutated antigen vaccine stimulated a sustained central memory $CD8^+$ T-cell response whereas the subsequent neoantigen vaccine preferentially mounted a T helper 1 (Th1)–like $CD4^+$ T-cell response (12). Collectively, these studies show that neoantigen vaccination is feasible for stimulating effector T cells that can home to the GBM microenvironment and provide the foundation for a personalized neoantigen vaccine–based approach for GBM. However, there remain a number of key factors that need to be evaluated related to the design of neoantigen vaccines to ensure an optimal platform that maximizes potential efficacy including neoantigen selection (including HLA class I vs. class II vs. both, HLA allelic representation per patient, correct number of clonal vs. subclonal targets, and criteria for ideal immunogenic candidate), vaccine platform (peptide, nucleic acid, viral, and dendritic cell) along with best adjuvant and ideal combination with other immunotherapies such as ICI, among others.

In this report, we directly addressed the issue of how to incorporate our understanding of intratumoral variant heterogeneity into neoantigen-targeting vaccine design. Specifically, we asked whether increasing the number of tumor regions sampled impacts the number and selection of neoantigens incorporated into a personalized vaccine by (i) providing a larger pool of candidate neoantigens and (ii) yielding information on their clonality and regional distribution. We have recently characterized the neoantigen landscape in GBM using multisector sequencing which revealed a striking degree of spatial heterogeneity (13). These findings suggested that designing personalized neoantigen vaccines in the setting of GBM based on single region sampling may not only be underrepresenting the broader pool of potentially immunogenic antigens but also not reflecting the clonal architecture sufficiently. Such considerations may have significant implications when it comes to evaluating the efficacy of a personalized vaccine approach in GBM because it may be critical to design "spatially encompassing" vaccine targeting approaches. Thus, to determine whether spatial heterogeneity can be effectively addressed by a personalized neoantigen vaccine, we performed multisector tumor sequencing and analysis to identify neoantigens in subjects with newly diagnosed, unmethylated MGMT GBM. We compared neoantigens across multiple regions to design and assess the safety, feasibility, and immunogenicity of a personalized neoantigen-based long peptide vaccine (NeoVax).

In this study, we report the findings of four subjects enrolled on the NeoVax clinical trial (NCT03422094). For each subject, multiple spatially distinct regions of resected primary GBM were characterized by whole-exome sequencing (WES), bulk RNA sequencing (RNA-seq), and nCounter® gene expression analysis. Matched peripheral blood mononuclear cells (PBMC) were collected from each subject before and after NeoVax to assess changes in T-cell receptor (TCR) clonal diversity and neoantigen reactivity. Our results demonstrate that multisector tumor sequencing can be readily incorporated into the workflow of personalized neoantigen vaccine design and increases the neoantigen candidate pool, which can be particularly important in low mutational burden tumors with high spatial heterogeneity like GBM. We also report immune responses raised by vaccination in three of the four subjects. Our results also demonstrate challenges in the implementation of long peptides in neoantigen-based vaccines including scalable production and a limit of the number of neoantigen sequences that can be reliably included, which may govern the clinical use of this platform.

Patients and Methods

Study design and overview

This study was registered on ClinicalTrials.gov as NCT03422094 and was conducted in accordance with Declaration of Helsinki and good clinical practice guidelines. All patients signed informed consent to an institutional tissue banking protocol and the study protocol, both of which were approved and monitored by the Institutional Review Board at Washington University School of Medicine. Patients were enrolled between May 2019 and May 2020. Key inclusion criteria included age 18 years and older, newly diagnosed central nervous system World Health Organization (CNS WHO) grade 4 GBM, and MGMT unmethylated based on a Clinical

Laboratory Improvement Amendment–certified assay. At the time of study conception and accrual, the WHO 2016 classification was used to define GBM; therefore, WHO grade 4 IDH–mutated astrocytomas were not excluded. However, all patients enrolled were IDH wild type as determined by next-generation sequencing. Additionally, the use of tumor-treating fields (TTF) was permitted while on study and was offered to all participants, but all subjects declined TTF therapy. Of note, bevacizumab was permitted as a steroid-sparing agent to treat symptomatic vasogenic edema or radiation necrosis while continuing to receive study drug. The use and timing of dexamethasone and bevacizumab for each subject are outlined in Supplementary Figs. S1 and S2.

At the time of resection, tumor tissue was sampled from two to three spatially distinct regions and flash frozen in individual vials as previously described (13). In brief, after surgical resection, punch biopsies were performed at two to three (depending on size of the tumor) spatially distant regions selected based on visual inspection. Distances were not specifically measured but an effort was made to select regions far apart from each other. An EDTA tube of peripheral blood was taken at the same time with PBMCs isolated by Ficoll gradient and cryopreserved to serve as a normal DNA comparator. Extraction of DNA was performed using the AllPrep DNA kit (QIAGEN), and RNA was isolated using the High Pure isolation kit (Roche Life Science). Following recovery from surgery, patients underwent a 6-week course of intensity-modulated radiotherapy per standard-of-care guidelines but without concurrent or adjuvant temozolomide. This is a precedent established by previous studies and multiple ongoing clinical trials in unmethylated MGMT GBM in which chemotherapy can be safely omitted in subjects with unmethylated MGMT GBM based on the lack of efficacy and potential negative impact on immune status (4). Approximately 4 weeks after completion of radiotherapy, the time frame within which adjuvant temozolomide and/or TTF would otherwise generally be started, NeoVax could be initiated once manufacturing was completed. NeoVax was given on days 1, 8, 15, and 22 of cycle 1 (priming phase) then on day 1 of each subsequent 28-day cycle (boosting phase). Each NeoVax was designed to contain up to 20 synthetic long peptides (SLP) divided into a maximum of four pools. SLPs were manufactured by Neon Therapeutics in collaboration with Creosalus. Each pool of NeoVax was co-administered with 1.5 mg of poly-ICLC (Hiltonol) and subcutaneously injected into one of the four limbs (right axilla, left axilla, right inguinal, and left inguinal). Nivolumab was provided by Bristol Myers Squibb.

WES and variant calling

Exome sequencing libraries were prepared using the NEBNext Ultra II FS DNA library prep kit (New England BioLabs). Target enrichment was first performed by hybrid capture using the xGen Exome Research Panel (#10005153) combined with the Cancer-Enriched Panels–Tech Access panel (Integrated DNA Technologies). The xGen Exome Research Panel targets 19,433 genes with a total probe coverage encompassing 39 Mb of genomic space. The Cancer-Enriched Panels–Tech Access panel provides an additional 1,855 probes that enrich for cancer-associated gene regions. Libraries were generated using the NEBNext Ultra II FS Kit, and paired end 151 bp reads were sequenced on the NovaSeq6000 to aim for 100× coverage in blood and 250× in tumor samples. Alignment to the human reference genome build GRCh38 and secondary analyses were performed using our previously published pipeline (14). Somatic variants were called using MuTect2 (RRID:SCR_000559). Somatic nonsynonymous single-nucleotide variants and small insertions or deletions (indels) were filtered for quality (site quality $\geq$ 100), population frequency (gnomAD population reads), minimum tumor variant allele frequency (VAF) $\geq$2%, and gene location within a coding or splice site ($\leq$3 bps) region. Variants passing all the aforementioned filters were manually reviewed in Integrated Genomics Viewer.

Neoantigen prediction

Clinical HLA class I typing was performed on normal comparator tissue obtained from blood-derived PBMCs by Histogenetics to two-field resolution. A variant call format (VCF) file was generated for each tumor region sample that contained all passing somatic variants annotated with Ensembl VEP (RRID:SCR_002344) using the parameters −everything, −flag_pick, and −plugin (Wildtype and Downstream). The VCF was further annotated for pVACseq according to pVACtools documentation (version 3.1.2). This VCF was used as input for a containerized version of pVACtools (15) to predict and annotate likely neoantigens (16). Briefly, using the submodule, "pvacseq run," we performed peptide/MHC binding affinity predictions with class I algorithms NetMHC and NetMHCpan. For this analysis, to be designated as a candidate neoantigen, a variant must have been validated in the WES analysis, have a best mutant (MT) IC_{50} <500 nM, an RNA transcript per million (TPM) >1, and (tumor RNA depth × RNA VAF) $\geq$3. The final neoantigens included in the NeoVax for each subject were those that were synthesized and soluble during manufacturing.

RNA-seq analysis and immune microenvironment profiling

Tumor RNA was subjected to DNase treatment and ribodepletion prior to library construction using NEBNext Ultra II Directional RNA library prep kit for Illumina (New England BioLabs). Paired end 151 bp reads were generated on the NovaSeq6000 to generate for a minimum of 80 million reads per sample; reads were aligned to the human genome reference sequence build GRCh38. Alignment was performed using a custom in-house pipeline and the splice-aware aligner STAR (RRID:SCR_004463). The Salmon tool (RRID:SCR_017036) was used to quantify transcript abundance from the tumor RNA-seq reads generated. To quantify tumor-infiltrating immunocyte populations in the GBM regional samples, we used the publicly available algorithm CIBERSORTx (RRID:SCR_016955), wherein the Salmon counts were referenced against the LM22 data set, a signature matrix file of 547 genes that accurately distinguish 22 mature human hematopoietic populations isolated from peripheral blood or *in vitro* culture conditions. Relative immunocyte proportions reported as percentages were plotted in R version 4.1.1 using ggplot2 (RRID:SCR_014601).

TCR repertoire sequencing

Genomic DNA from the peripheral blood pre- and post-NeoVax for subjects 1 to 3 and post-NeoVax tumor biopsy for subject 3 were submitted to Adaptive Biotechnologies for sequencing of the complementarity-determining region 3 (CDR3) of the TCR-β chain. Analysis was performed using the immmunoSEQ Analyzer 3.0. Specifically, the pairwise scatter plot, differential abundance, and scatterplot with annotation tools were used, and the values displayed were productive frequency and amino acid sequence. Productive frequency is the frequency of a given TCR nucleotide sequence to produce a functional peptide and can be used to track clonal expansions. Program default statistical methods and cut-offs were used.

ELISPOT assay

To measure T-cell responses against vaccinated neoantigens, two approaches were taken—direct *ex vivo* stimulation and *in vitro* expansion. For direct *ex vivo* stimulation, we adopted a previously published method (11). Briefly, $CD8^+$ and $CD4^+$ cells were isolated from PBMCs using sequential magnetic bead-based positive selection kits (STEMCELL Technologies). Approximately 100,000 double-negative autologous PBMCs were incubated on pre-coated human IFN-γ ELISPOT plates (Cellular Technology, Ltd.) with 10 μmol/L of indicated peptide(s) (GenScript) plus ~400,000 $CD8^+$ or $CD4^+$ PBMCs for 18 to 20 hours at 37°C. Each peptide pool was composed of either the full-length peptide encoded in the vaccine or pools of 9- to 11-mers corresponding to the predicted high affinity minimal epitopes for each patient's HLA alleles. Plates were analyzed using the C.T.L. ImmunoSpot kit (Cellular Technology, Ltd.). This approach allows for distinction between CD8 and CD4 neoantigen-specific T-cell responses but requires a larger volume of PBMCs to be collected, typically an apheresis product, to obtain sufficient T cells to test all peptides in biological replicates. As such, this assay could not be performed on subject 3 due to a lack of available PBMCs. Therefore, we also used an *in vitro* expansion assay which could be applied to samples with the smaller volume of PBMCs available and allowed higher sensitivity detection of antigen-specific responses, albeit without the ability to accurately distinguish $CD8^+$ and $CD4^+$ T-cell reactivity due to a lack of selection (17). In brief, on day 1, 1×10^6 PBMCs were cultured with 10 μmol/L each of corresponding neoantigen peptide pools. Each peptide pool was composed of the full-length peptide encoded in the vaccine along with pools of 9- to 11-mers comprising predicted high affinity minimal epitopes corresponding to patient-specific HLA alleles. On day 4, media were supplemented with recombinant human IL2 (Peprotech) to a final concentration of 50 IU/mL. Fresh IL2 containing media were added every 3 days thereafter. On day 12, cells were harvested and washed twice and allowed to rest overnight without peptide or IL2. On day 13, cells were restimulated with 1×10^5 autologous T-cell depleted PBMCs (STEMCELL Technologies) and respective neoantigen minimal epitope peptide pools, the full-length peptide, or DMSO in a human IFNγ ELISPOT plate (ImmunoSpot). The ELISPOT plate was developed 18 to 24 hours later. Experiments were performed with duplicate or triplicate wells, and biological replicates were performed at least twice. A positive neoantigen response to vaccination was defined as (i) a minimum of 20 IFNγ producing spots per well on average; (ii) a statistically significant increase compared with DMSO control; and (iii) a statistically significant increase compared with prevaccination time point. Student *t* test was performed to determine statistical significance ($P < 0.05$).

IHC

Histologic assessment of slides with the highest density of inflammatory cells was performed using hematoxylin and eosin–stained sections. IHC for CD8 (Ventana, SP57 clone, prediluted) and CD3 (Ventana, 2GV6 clone, prediluted) was performed using a Ventana IHC autostaining platform on the selected blocks. Three CD8 and CD3 hotspot areas (0.22 mm^2) were identified and manually counted for the pre- and postvaccination specimens. Student *t* test was performed to determine statistically significant ($P < 0.05$) differences between mean staining density pre- and postvaccination.

nCounter® targeted expression

RNA (150 ng) extracted from a normal human brain reference (Thermo Fisher Scientific; AM7962) and from subject 3 pre- and post-NeoVax tumor regions were assayed with the nCounter® CAR-T Characterization Panel from NanoString. RCC files were uploaded to the NanoString ROSALIND analysis platform and counts were normalized and differential gene expression was performed using the platform software. Log_2 normalized and *P*-values were exported and plotted using pheatmap in R version 4.1.1 (RRID:SCR_016418). Categorical associations of differentially expressed genes were determined by comparing differentially expressed genes to the CAR-T Characterization Panel categorical gene assignments provided in the CAR-T annotation files by NanoString (RRID:SCR_023424). Calculated percentages were plotted in R version 4.1.1 using ggplot2 (RRID:SCR_014601).

Data availability

The RNA-seq and NanoString gene expression data presented in this publication have been deposited in NCBI's Gene Expression Omnibus and are accessible through Gene Expression Omnibus Series accession number GSE238012. The WES presented in this publication has been deposited in NCBI's Sequence Read Archive and is accessible through BioProject ID PRJNA999679.

Results

Trial overview

The trial was a pilot study to assess the safety, feasibility, and immunogenicity of a personalized neoantigen peptide vaccine (NeoVax) in patients with GBM following radiotherapy. A total of four subjects were enrolled and reported herein. Subjects were to receive nivolumab starting at time of disease progression; however, due to the rapid functional decline at time of tumor progression observed in subjects 1, 2 and 4, as well as the lack of true tumor progression observed in subject 3, we were not able to fully assess the immunologic effects or potential clinical benefit of nivolumab following NeoVax within the scope of this cohort. A detailed outline of each subject's clinical course is summarized in **Fig. 1A** and Supplementary Figs. S1 and S2. Information on the representatives of study participants is reported in Supplementary Table S1. Therefore, the data reported here focus on the development and immunogenicity of NeoVax only.

Safety and feasibility

The primary endpoint of the study was to determine the safety and feasibility of generating and administering a personalized neoantigen synthetic long peptide (SLP)–based vaccine. Of the four subjects enrolled on the study, three received NeoVax and were eligible for safety assessment. There were no unexpected toxicities. No subject experienced a severe adverse event (AE; CTCAE v4.0 grade 3 or greater AE). The most common treatment-related AE reported was grade 1 or 2 injection site reactions (pain, bruising, swelling, and redness) and malaise. Both subjects 1 and 3 developed grade 2 symptomatic vasogenic edema (seizure and worsening right sided weakness, respectively) while receiving NeoVax, which improved with bevacizumab. All four patients were evaluated for the feasibility endpoint. Feasibility was defined as (i) the ability to manufacture a corresponding personalized neoantigen-based SLP vaccine, (ii) the ability to administer the personalized peptide vaccine by 4 weeks of completing radiotherapy, the time when adjuvant chemotherapy would generally be started, and (iii) the ability to identify candidate HLA class I neoantigens in peripheral blood following NeoVax administration.

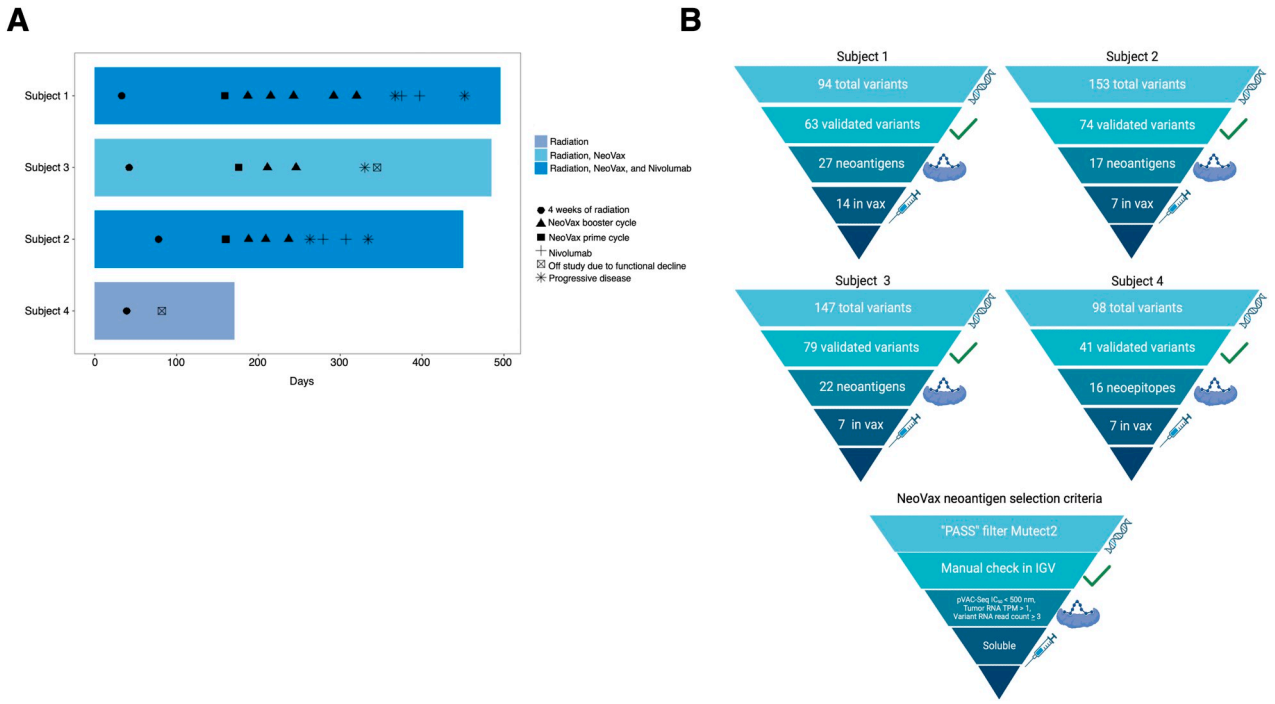

Figure 1.

Summary of patients. **A,** Swimmer plot of clinical courses for subjects 1–4. **B,** Selection criteria for neoantigens that were included in the personalized NeoVax. IGV, Integrative Genomics Viewer; TPM, transcript per million; variant RNA read count = [tumor RNA depth × RNA VAF]. (Adapted from an image created with BioRender.com.)

Vaccine design and production

Candidate neoantigens were identified and prioritized by pVAC-seq analysis, an algorithm that incorporates variant calls from tumor and normal whole-exome sequencing (WES) variant expression inferred from tumor RNA-seq and patient-specific HLA class I peptide binding affinity predictions (15). For each subject, candidate neoantigens were selected based on an HLA class I affinity binding score, IC_{50}, of less than 500 nM; a tumor RNA TPM value of greater than 1; and a variant RNA read count of 3 or greater (variant RNA read count = tumor RNA depth × RNA VAF). As outlined in **Fig. 1B**, candidate HLA class I neoantigens that met these criteria were identified in all patients, ranging from 16 to 27. On average, 32.9%, or roughly one out of three, neoantigens were considered good candidates for NeoVax inclusion due to meeting the aforementioned criteria. This is an encouraging finding when considering the feasibility of identifying sufficient neoantigens for vaccination in similarly low mutation burden tumors.

SLPs were then designed for each of the candidate neoantigens. Although the clinical trial protocol limited the number of neoantigen targets within any single polyvalent vaccine to 20, more than 20 neoantigens were selected for SLP manufacturing for some patients due to the assumption that up to 50% of peptides either could not be synthesized or would not be soluble, and thus, not be included in the final NeoVax product (11). Indeed, of the initial 27 neoantigens selected for subject 1, 14 were manufactured, soluble, and included in the final NeoVax product. Similarly, seven neoantigens each were ultimately manufactured for subjects 2 to 4 out of an initial 17, 22, and 16 selected neoantigen candidates, respectively (**Fig. 1B**; Supplementary Tables S2-S4). In total, 43% of selected candidate neoantigens were successfully manufactured and formulated into a clinical-grade SLP vaccine product consistent with our initial assumption of a 50% successful production rate. Neoantigen-containing peptides included in each NeoVax are listed in Supplementary Table S4. Of note, all subjects had a mutation in *PTEN*; however, only subject 2 had a PTEN-derived neoantigen included in the final NeoVax product. Subject 2 also had a BRAF V600E–derived neoantigen included in the NeoVax formulation.

We next assessed the parameter of "time to administration of NeoVax" for each patient. Total production time took an average of 164 days from the date of tumor resection to administration of the first NeoVax dose. However, the goal was to administer the first dose of the vaccine at 4 weeks post-completion of radiotherapy, which corresponds to the time when adjuvant chemotherapy would generally be initiated. Specifically, for subjects 1 to 3, NeoVax was administered 85, 51, and 94 days after the completion of radiotherapy, respectively. For subject 4, the NeoVax product was delivered to our institution 66 days from the completion of radiotherapy, although this patient did not receive the vaccine. In summary, these times to vaccination did not meet the feasibility endpoint of 4 weeks, and thus the SLP neoantigen vaccine platform was assessed as harboring feasibility issues from a manufacturing turnaround perspective which would need to be abbreviated if this approach were to be adopted to GBM moving forward.

Clinical outcomes

As summarized in **Fig. 1A** and Supplementary Figs. S1 and S2, subject 1 was a 51-year-old male who completed the priming phase of NeoVax along with five cycles of booster vaccinations before

disease recurrence and subsequently received two cycles of nivolumab before passing away 497 days from time of diagnosis due to progressive disease. Subject 2 was a 62-year-old female who completed the priming phase of NeoVax followed by three cycles of booster vaccinations before disease recurrence and subsequently received two cycles of nivolumab followed by dual BRAF/MEK inhibitor therapy without response and ultimately passed away 457 days from the time of diagnosis due to disease progression. Subject 3 was a 62-year-old female who completed the priming phase of NeoVax and two cycles of booster vaccinations before coming off study due to functional decline. A second intracranial biopsy was performed to evaluate for possible tumor recurrence, but pathology was reported as quiescent residual glioma (no mitoses or increased cellular density) with marked treatment effect comprised predominantly of radiation necrosis. Of note, subject 3 initially presented with significant right sided weakness that persisted after surgery. These symptoms initially worsened after initiating NeoVax therapy and were thought to be due to increased vasogenic edema noted on magnetic resonance imaging, but symptoms continued to worsen despite radiographic improvement of edema and necrosis following bevacizumab therapy. Therefore, she was enrolled in hospice and passed away 486 days after initial diagnosis. Subject 4 was a 52-year-old male whose post-op course was complicated by left sided hemiparesis and whose functional status declined rapidly following radiotherapy precluding vaccine administration or further treatment. He ultimately entered hospice and passed away 195 days from the time of diagnosis. Progression-free survival for subjects 1 to 3 was 12, 9, and 15 months, respectively (**Fig. 1A**; Supplementary Figs. S1 and S2). Although subject 1 had 14 neoantigens included in their vaccine and subjects 2 and 3 only had 7, we did not see a difference in the clinical outcome, likely due to the small size of the cohort, thus we are unable to definitively assess a potential correlation.

Multisector sampling and neoantigen distribution: considerations for designing spatially targeted vaccines

Schaettler and colleagues and others have highlighted the importance of multisector sampling and analysis in vaccine development for GBM as it relates to both neoantigen discovery and selection (13, 18). Specifically, they noted that the breadth and distribution of candidate neoantigens can only be wholly appreciated through sampling of multiple spatially distinct tumor regions due to the inherent subclonal architecture of high-grade glioma. Therefore, a fundamental aspect of this study was to integrate this concept of candidate neoantigen identification and selection by incorporating multisector sampling into the design of "spatially encompassing" vaccines.

To characterize the genomic heterogeneity of the four subjects reported here, spatially distant regions of the resected tumor tissue were sampled: three from subjects 1 to 3 and two from subject 4 (regions limited by resection specimen size; **Fig. 2A**). As depicted in **Fig. 2B**, WES was performed on each individual resected tumor region at an average coverage depth of 267× (range 237×–306×) and on the PBMCs from the paired peripheral blood to serve as a normal comparator at an average coverage depth of 223× (range 183×–258×). After MuTect2 somatic variant calling and manual confirmation, we identified a total of 63 unique variants [both single-nucleotide variants and insertions/deletions (indels)] for subject 1, 58.7% (37/63) of which were shared among all three regions (clonal), 17.5% (11/63) were shared between one or more regions (subclonal shared), and 23.8% (15/63) of which were exclusive to a given region (subclonal private). Subject 2 had a total of 74 unique variants, 71.6% (53/74) of which were clonal, 5.4% (4/74) were subclonal shared, and 23% (17/74) were subclonal private. Subject 3 had a total of 79 unique variants, 72.2% (57/79) of which were clonal, 5.1% (4/79) were subclonal shared, and 22.8% (18/79) were subclonal private. Subject 4 had a total of 41 unique variants, 61% (25/41) of which were clonal and 39% (16/41) were subclonal private (**Figs. 2C** and **3A**; Supplementary Table S2). Neoantigens included in the NeoVax for each subject are highlighted in the call out boxes (**Fig. 3A**).

These results are consistent with the previous observations by Schaettler and colleagues demonstrating that although the majority of variants are shared among all regions sampled, there remains a significant number of variants (25%–40%) that are regionally restricted (13). As expected, clonal and subclonal shared variants had the highest VAF in all subjects (**Fig. 3B**; Supplementary Table S2) and were used to guide neoantigen selection for each subject's NeoVax design. Subject 1 had 18 clonal, 5 subclonal shared, and 4 subclonal private neoantigens selected, yet only 9, 2, and 3, respectively, were successfully manufactured. Subject 2 had 16 clonal and 1 subclonal shared neoantigen(s) selected with 7 clonal neoantigens successfully manufactured. Subject 3 had 19 clonal, 1 subclonal shared, and 2 subclonal private neoantigens selected, of which 6 clonal and 1 subclonal private neoantigen(s) were successfully manufactured. Subject 4 had 14 clonal and 2 subclonal private neoantigens selected, but only 6 clonal and 1 subclonal private neoantigen(s) were successfully manufactured (**Figs. 1B** and **3A**; Supplementary Table S4).

TCR clonotypic diversity following NeoVax

To evaluate changes in T-cell receptor (TCR) repertoire diversity of subjects before and after NeoVax (subject 4 was not included in the analysis due to lack of vaccination), we performed immunoSEQ (Adaptive Biotechnologies) on paired PBMCs from specimens collected prior to the first dose of NeoVax and prior to cycle 4 (the third booster vaccine). If the NeoVax induced variant-specific T-cell clonal expansion, we would expect to see an emergence of higher frequency clones in the circulating peripheral blood after vaccination. The immunoSEQ method amplifies the V–D–J regions from isolated peripheral blood genomic DNA and uses the TCR β-chain CDR3 as a unique barcode to track the frequency of individually expanded productive TCR clones. We used the immunoSEQ Analyzer program to calculate Productive Simpson Clonality scores, the square root of Simpson's diversity index (range from 0–1, with values approaching 1 representing a monoclonal sample and values approaching 0 representing a polyclonal sample), for each sample. Subjects 1 and 2 had similar scores before and after vaccination, whereas subject 3 had an increase by a fold change of two after vaccination, which is indicative of clonal expansion (Supplementary Fig. S3). We used the differential abundance tool from immunoSEQ Analyzer to identify TCR clones that have a significant increase (P-value $\leq$ 0.05 and fold change $\geq$2 and <infinity) in frequency after vaccination (19, 20). Subjects 1, 2, and 3, had a total of 12, 24, and 66 clones, respectively, that met these criteria (**Fig. 4A–C**; Supplementary Tables S5 and S6). The publicly available TCRMatch database from the Immune Epitope Database and Analysis Resource was used to screen the expanded clones for known paired antigen targets. TCRMatch scores between 0 and 1, with 1 indicating an exact match with the input CDR3β sequence. A threshold of $\geq$0.97 was used as recommended by the program (21). This analysis revealed 75% (9/12), 83% (20/24), and 83% (55/66) of the CDR3β sequences, respectively for subjects 1-3, were not found in the

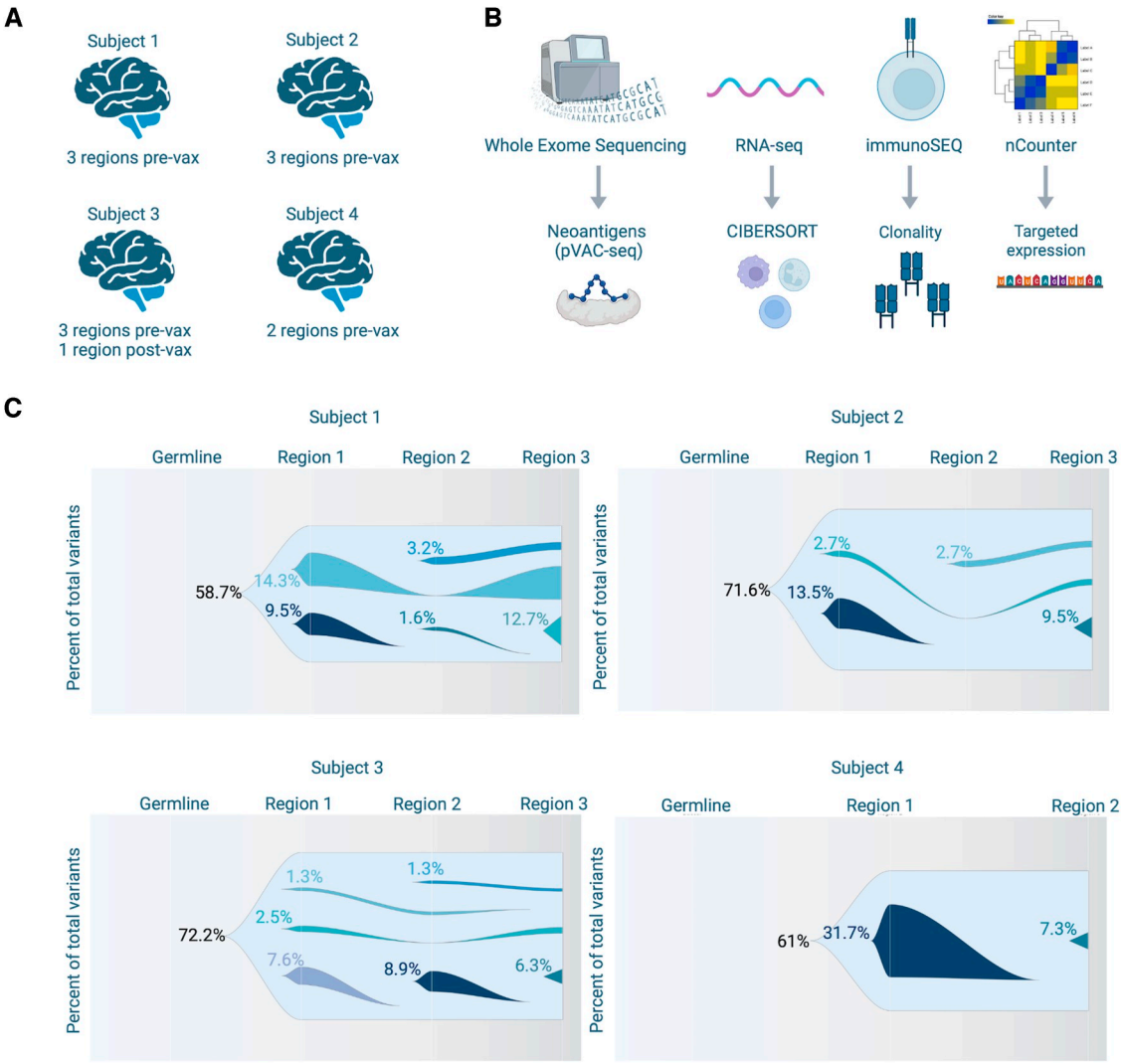

Figure 2.

Multisector tumoral sampling and molecular characterization. **A,** Schematic of subjects included in cohort and tumor regions sampled for downstream analysis. **B,** Schematic of molecular characterization and analyses performed on the cohort. **C,** Fish plots representing the percent of all total validated variants per region in each subject. (Adapted from an image created with BioRender.com.)

database, suggesting they are not specific to any known viral or cancer antigen, further supporting they may be patient variant–specific. The remaining clones were identified to respond to known antigens from common viruses such as SARS-CoV2, Epstein–Barr virus, and human cytomegalovirus (Supplementary Table S6).

Reactivity to neoantigens included in the personalized NeoVax vaccines was assessed in peripheral blood collected pre- and post-vaccination using IFNγ ELISPOT. Similar to our previous work, initial response assessment was performed with direct *ex vivo* stimulation on select $CD8^+$ and $CD4^+$ T cells. Of note, this analysis could only be performed on subjects 1 and 2 as there was insufficient peripheral blood collected from subject 3 following vaccination. In subject 1, we observed significant $CD8^+$ T-cell reactivity to the pool of NDFIP2 peptides (**Fig. 4D**), and to the full-length peptides of PLXNB1, PROSER1, and SPEG by $CD4^+$ T cells at the postvaccination time point (**Fig. 4E**). No significant reactivity to these respective neoantigens was seen in the prevaccination sample (**Fig. 4F** and **G**). Representative images of counted IFNγ spots are shown in Supplementary Fig. S4. Conversely, in subject 2, we did not observe significant reactivity to any of the corresponding neoantigens at the postvaccination time point by either $CD8^+$ or $CD4^+$ T cells (data not shown). To determine if additional responses could be detected following *in vitro* expansion, we stimulated PBMCs from pre- and postvaccination time points with corresponding peptides and IL2 for 12 days (see Materials and Methods) prior to restimulation and analysis by IFNγ ELISPOT. We found a statistically significant increase in IFNγ producing T cells at the postvaccination time point to the following neoantigens: ELFN1, PLXNB1, and PROSER1 for subject 1 (**Fig. 4H** and **I**); BRAF, COL27A1, and DPYSL5 for subject 2 (**Fig. 4J** and **K**); and C19orf48 and SAMD9L for subject 3 (**Fig. 4L** and **M**). Reactivity to these neoantigens was seen following restimulation with the full-length peptide only with

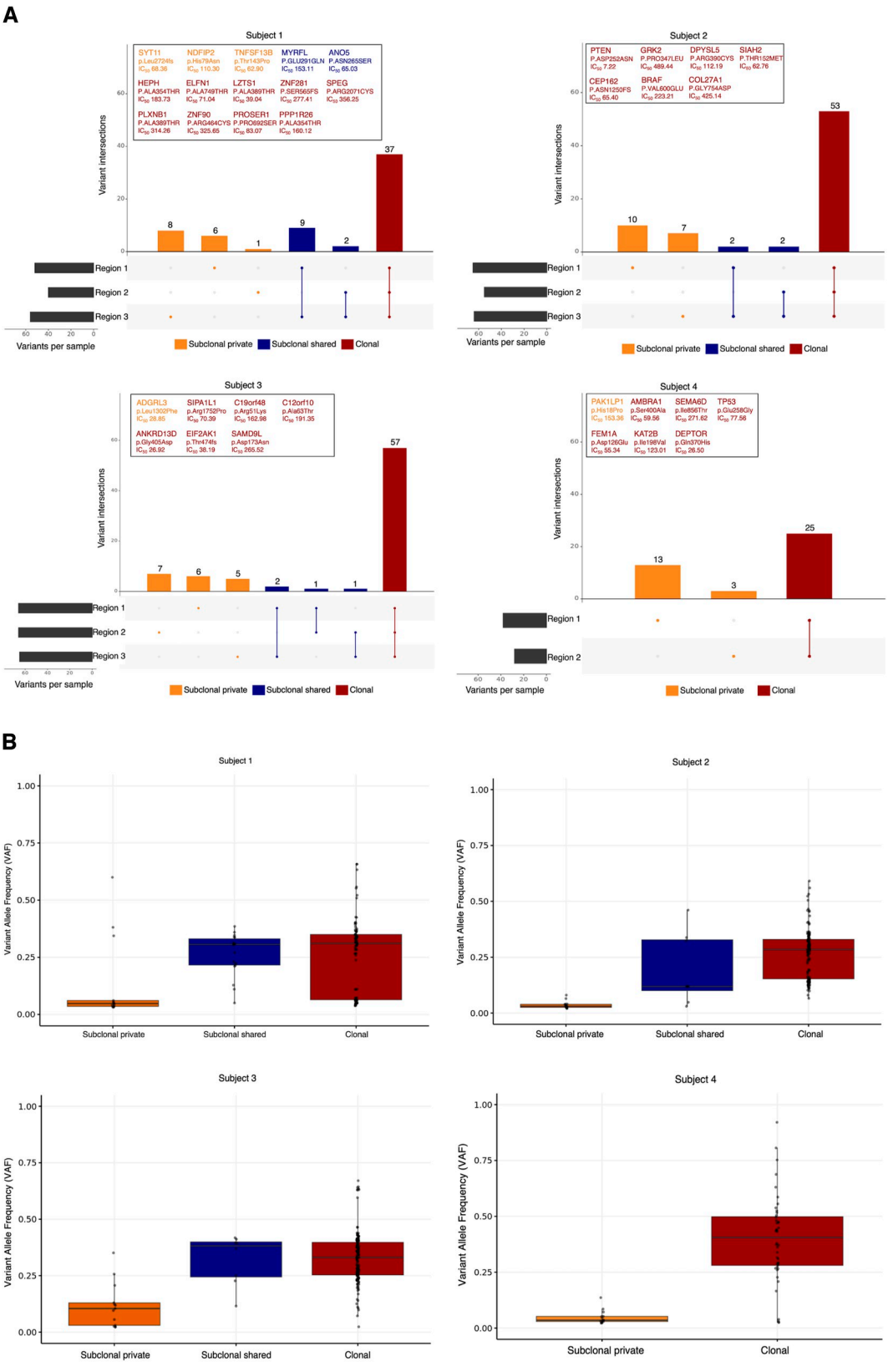

Figure 3.

Spatial distribution of variants. **A,** UpSet plot of the variant distribution of each subject grouped by shared regions. Box highlights variants included in NeoVax. **B,** DNA VAF of clonal, subclonal shared, and subclonal private variants for each subject.

the exception of COL27A1 in which reactivity was seen to both the full-length peptide and pooled minimal epitope peptides suggesting these responses were biased toward CD4 T-cell reactivity. It should be noted that due to limited clinical samples, further deconvolution of neoantigen reactivity to more precisely define the immunogenic minimal epitopes or CD8/CD4 specificity could not be completed. Together, these results suggest that NeoVax did significantly enhance reactivity to a subset of patient-specific neoantigens.

Molecular characterization of a post-NeoVax tumor microenvironment

Due to functional decline and to rule out disease progression, subject 3 underwent a biopsy post-NeoVax of a residual area of contrast enhancement at the site of prior tumor resection, providing us a unique opportunity to characterize the tumor microenvironment following vaccination. Histopathologic examination of the biopsy specimen demonstrated radiation necrosis with residual quiescent glioma cells, suggesting no active disease recurrence to account for the radiographic and clinical findings. WES of the specimen revealed variants found in the residual tumor cells were shared with the pre-NeoVax regions (**Fig. 5A**; Supplementary Table S2), albeit at a lower DNA VAF due to the lower tumor content (estimated by pathology to be less than 10%; **Fig. 5B**; Supplementary Table S2). SciClone analysis, a tool to track clonal evolution of tumor cells, revealed four populations in the post-NeoVax biopsy that were also shared between all pre-NeoVax tumor regions (**Fig. 5C**; ref. 22). However, consistent with **Fig. 5B**, the DNA VAFs of these populations were lower post-NeoVax, suggesting that these persistent tumor cells did not represent the emergence of a minor subclone from the initial tumor specimen as has been seen previously (11). Given that these post-NeoVax subclones were present in the initial tumor sample, they were likely targeted by NeoVax. Indeed, a majority of subject 3's NeoVax neoantigens were present in populations 2 to 4 (**Fig. 5C**). We have previously described the downregulation of neoantigens in tumor cells that persist following vaccination (11) as a potential mechanism of immune escape. To explore if a similar mechanism of resistance is observed in this patient, we plotted the expression values (transcript per million, TPM) of the genes harboring all 79 validated variants for subject 3 and noted a broad downregulation in expression in the postvaccine specimen. When sub-setting for only the genes harboring the neoantigens targeted in the patient's NeoVax, there was a uniform downregulation in the post-vax biopsy (Supplementary Fig. S5; Supplementary Table S7). Of note, there was a small population of genes upregulated after vaccination, but these 20 genes were not significantly associated with any specific Gene Ontology pathway. Collectively, these data support our previous finding of downregulated antigen expression in persistent tumor cells which may account for lack of recognition by antigen-specific T cells. However, the potential contribution of lower tumor cellularity accounting for this global lack of expression detected cannot be quantified.

To investigate changes in the immune repertoire after NeoVax, the immunoSEQ assay was performed on DNA extracted from the post-NeoVax biopsy. The immunoSEQ Analyzer program was used to calculate the Productive Simpson Clonality score for this sample. The post-NeoVax biopsy had a clonality score of 0.0508, which when compared with the clonality scores of 0.0389 and 0.0848 from the PBMC pre- and postvaccination, respectively, shows a 1.3× increase in clonality in the tumor microenvironment after vaccination. We saw an increase of 1.1× when compared with the pre-vaccination tumor regions (Supplementary Fig. S3). To characterize the TCR repertoire in the tumor microenvironment post-NeoVax, we used the immunoSEQ Analyzer program to identify clones found in the PBMC samples that were also present in the post-vaccination biopsy. Of note, out of the 66 CDR3β sequences with a significant increase in the blood after vaccination, 60 were present in the post-NeoVax tumor biopsy sample at a frequency greater than zero and not found in the TCRMatch database (**Fig. 5D**; Supplementary Tables S5 and S6; ref. 21), suggesting an influx of $CD8^+$ T cells from the circulating blood to the brain, although we cannot exclude a possible contribution of blood contamination in the post-NeoVax tumor biopsy. Moreover, using CIBERSORTx to deconvolute the cell populations within the post-NeoVax tumor biopsy RNA-seq, we observed a relative increase in $CD8^+$ T cells. The algorithm predicted an infiltration of 11.08% $CD8^+$ T cells compared with the average of 0.65% in the pre-NeoVax tumor regions (**Fig. 5E**; Supplementary Tables S7 and S8). Notably, although peptide-based vaccines tend to generate a greater CD4 T-cell response over CD8 (10, 12), we did not observe an increase in $CD4^+$ T-cell frequency. The CIBERSORTx algorithm predicted an infiltration of 12.47% in the post-NeoVax biopsy compared with an average of 17.58% in the pre-NeoVax tumor regions of specifically CD4 memory resting T cells (Supplementary Tables S7 and S8). Immunohistologic assessment of pre- and post-NeoVax biopsy tissue was also consistent with a modest, but not significant (P-value = 0.2659), increase in $CD8^+$ T cells in the postvaccination sample by manual count of three averaged hotspot areas (113 vs. 55 cells/mm^2; Supplementary Fig. S6; Supplementary Table S9). Due to $CD4^+$ IHC staining on other immunocytes (histiocytes and other monocytic lineage cells), we could not use this assay to directly quantify $CD4^+$ T cells in the tumor samples. Instead, we stained for CD3 as a surrogate for the entire mature T-cell population and again found a modest, but not significant (P-value = 0.7635) increase in $CD3^+$ cells in the postvaccination sample by manual count of three hotspot areas averaged (129 vs. 137 cells/mm^2; Supplementary Fig. S6; Supplementary Table S9).

To further elucidate the expanded $CD8^+$ T-cell clones, we ranked the unique 60 CDR3β sequences shared between the post-NeoVax PBMC and tumor biopsy sample by abundance in the tumor biopsy. Eight of the top 10 tumor biopsy clones were also found in the top 10 expanded clones in the post-NeoVax PBMC sample (Supplementary Fig. S7). We also calculated the ratio of CDR3β abundance in the post-NeoVax tumor biopsy versus the PBMC sample and ranked these ratios from smallest to largest, with the lower ratio representing clones of similar abundance. Seven of the top 10 post-NeoVax tumor biopsy clones were present in the top 20 lowest ratios (Supplementary Fig. S8). Collectively, these data suggest an expansion of vaccine stimulated, tumor-directed effector T cells; however, strong conclusions cannot be made in the absence of more definitive analyses such as tetramer staining or isolating TCR pairs to perform validation assays of neoantigen reactivity.

To characterize more specifically the gene expression changes in the tumor microenvironment associated with T cells, we used the targeted and highly sensitive NanoString nCounter® system to detect and count transcripts in a panel of 722 genes associated with CAR-T cells. The CAR-T Characterization Panel includes genes associated with T-cell diversity, phenotype, metabolic fitness, exhaustion, persistence, and activation and is, therefore, well-suited to explore immunotherapeutic effects more broadly. Seventy-six genes were differentially expressed by a fold change of at least 1.5, although none reached a level of significance. In total, 43% (33/76) were downregulated and 57% (43/76) were upregulated in post-NeoVax compared with pre-NeoVax (**Fig. 6A**; Supplementary Table S10). Among the top differentially expressed genes, we identified an

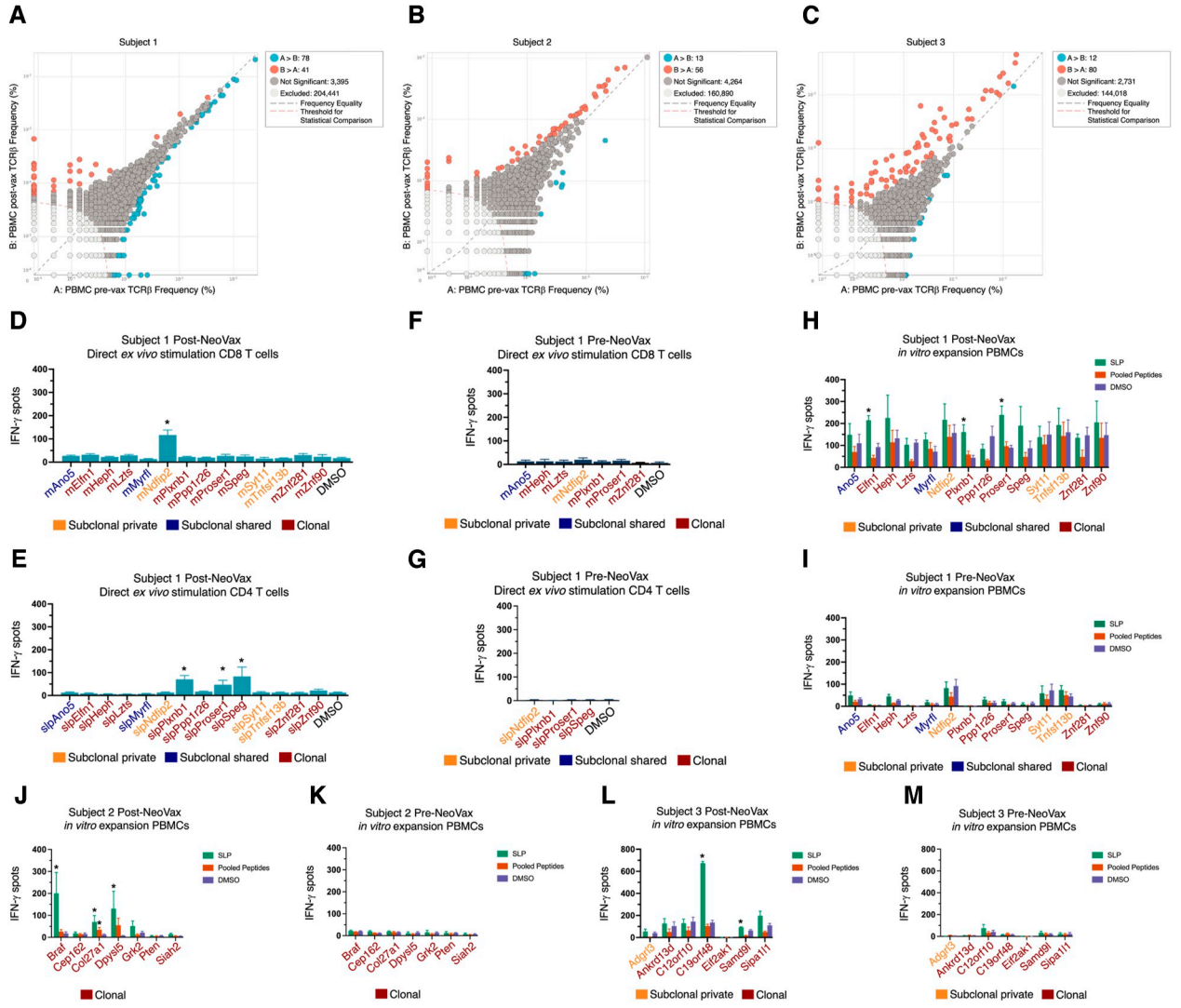

Figure 4.

T-cell characterization. **A–C,** immunoSEQ Analyzer differential abundance analysis displayed in pairwise scatter plots are shown for subjects 1, 2, and 3, respectively. The frequency of productive TCRβ rearrangements (clones) from the peripheral blood before and after NeoVax is compared. No data are available for subject 4 because they did not receive NeoVax. **D–M,** Bar graphs displaying IFNγ spots from IFNγ ELISPOT assays. Experiments were performed with duplicate or triplicate wells, and biological replicates were performed at least twice. *, $P < 0.05$ (Student *t* test) between pre- and post-NeoVax responses. There were 84, 77, and 35 days between pre- and post-NeoVax peripheral blood collections for subjects 1, 2, and 3, respectively. **D,** Direct *ex vivo* stimulation on select $CD8^+$ T cells with minimal epitope peptide pools (m) or DMSO control for subject 1 post-NeoVax. **E,** Direct *ex vivo* stimulation on select $CD4^+$ T cells with SLPs or DMSO control for subject 1 post-NeoVax. **F,** Direct *ex vivo* stimulation on select $CD8^+$ T cells with minimal epitope peptide pools (m) or DMSO control for subject 1 pre-NeoVax. **G,** Direct *ex vivo* stimulation on select $CD4^+$ T cells with SLPs or DMSO control for subject 1 pre-NeoVax. **H–M,** *In vitro* expanded PBMCs from pre- and postvaccination time points stimulated with IL2 and corresponding SLPs (green bars), minimal epitope peptide pools (dark orange bars), or DMSO control (purple bars) for 12 days prior to restimulation and analysis for subjects 1, 2, and 3.

upregulation of *NFAT5* and *MAPK3* and a downregulation of *BATF3* and *TP53* (**Fig. 6B**; Supplementary Table S10). The differentially expressed genes were mapped to the categorical associations of genes included in the CAR-T Characterization Panel provided by NanoString. The top downregulated genes were assigned to known pathways and identified Myc targets, activation markers (*CD40L*, *CD69*, and *IL2RA*), and cell-cycle genes (**Fig. 6C**; Supplementary Table S10). The lack of active proliferation of tumor cells post-NeoVax is consistent with observations reported by Cloughesy and colleagues following neoadjuvant PD1 blockade in patients with recurrent GBM (23). NFAT, glutamine metabolism, and mTOR were identified to be the top upregulated pathways in the GBM microenvironment post-NeoVax (**Fig. 6D**; Supplementary Table S10). Upregulation of these pathways is associated with T-cell activation and fitness. Of note, as the pre-NeoVax samples were taken at time of diagnosis, the observed changes in T-cell and tumor biology cannot be solely attributed to NeoVax treatment as the relative contribution from surgery and/or radiation is not able to be determined. However, these analyses prior to adjuvant treatment can provide insights into the state of the endogenous immune

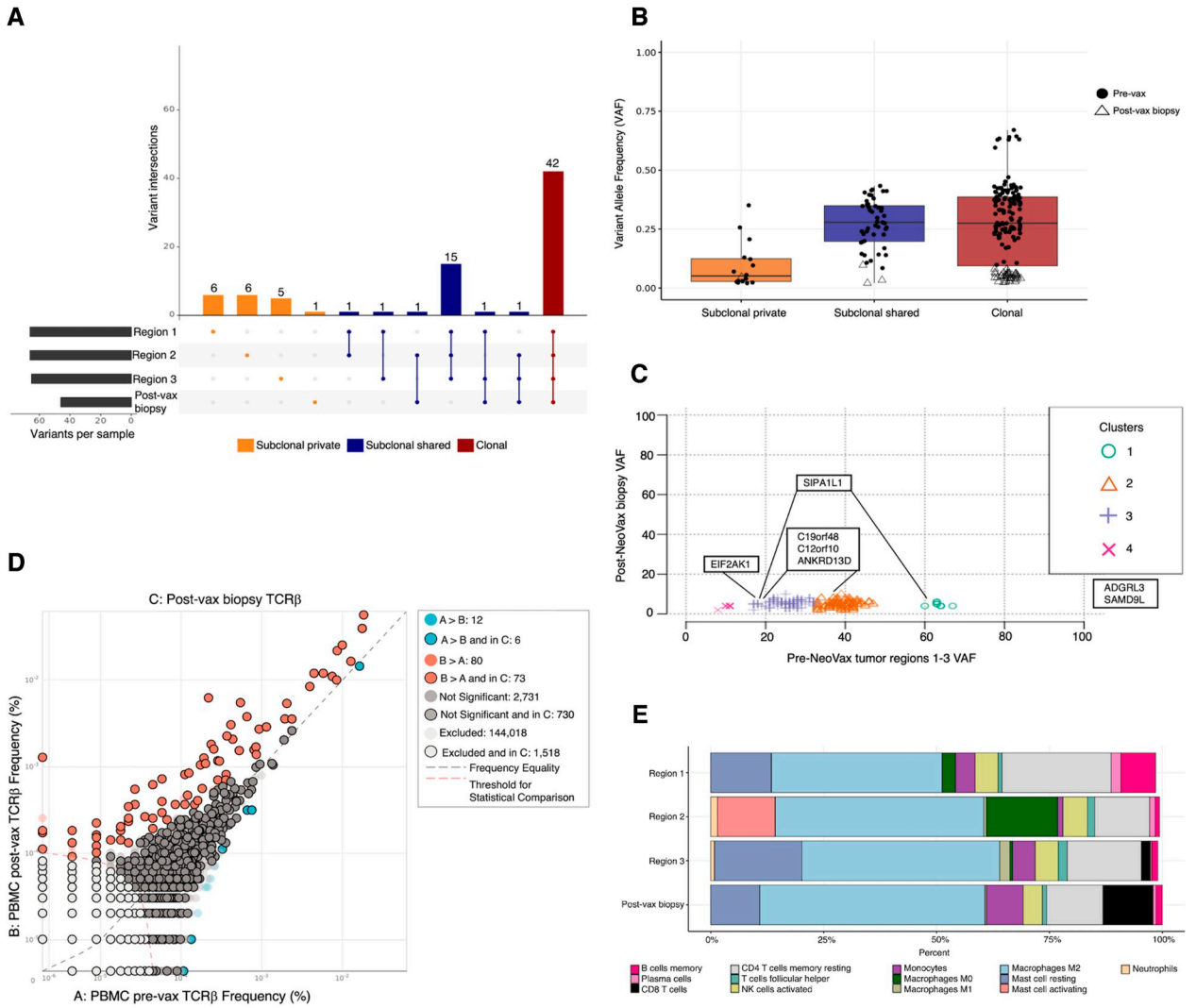

Figure 5.

Molecular and immunologic characterization of subject 3 post-NeoVax tumor biopsy. **A,** UpSet plot of the variant distribution grouped by shared regions with the inclusion of the post-NeoVax tumor biopsy sample. **B,** DNA VAF of clonal, subclonal shared, and subclonal private variants. Post-NeoVax tumor biopsy samples are highlighted by an open triangle symbol. **C,** SciClone plot of subclone populations present in pre- and post-NeoVax tumor samples. DNA VAF is displayed. Neoantigens included in subject 3's NeoVax and their cluster location are in the call-out boxes. ADGRL3 and SAMD9L did not map to one of the four clusters. **D,** immunoSEQ Analyzer differential abundance analysis displayed in pairwise scatter plot is shown. The frequency of productive TCRβ rearrangements (clones) from the peripheral blood before and after NeoVax is compared. The presence of the clones in the post-vax biopsy is indicated with a black outline. **E,** Percent of regional tumor-infiltrating immune cell types as deconvoluted by CIBERSORTx. Proportion of $CD8^+$ T cells are colored in black.

response. Nevertheless, the collective analyses of the post-NeoVax tumor biopsy sample and paired pre- and post-NeoVax peripheral blood suggests vaccination stimulated the clonal expansion of tumor-directed effector T cells.

Discussion

In this study, we demonstrate that incorporating multisector sampling in GBM increases the candidate pool of potentially targetable neoantigens while also providing information about the clonality and distribution of the neoantigens selected. Although our cohort was small and limited to only one post-NeoVax tumor sample, we were able to show that administration of up to six doses of NeoVax is safe and well tolerated. We provide preliminary data that suggest a clonal expansion of effector T cells following NeoVax that are responding to the neoantigens included in the vaccine. Moreover, these observed effects of NeoVax on the tumor and its immune microenvironment are encouraging and support the future development of cancer vaccine–based immunotherapies in GBM that will guide subsequent studies.

It is not unreasonable to think that the vaccine alone, without combination treatment approaches, may be insufficient to generate the antitumor immune response needed to mediate response to an aggressive malignancy like GBM. However, the rationale that vaccination can induce a neoantigen-specific T-cell response that may be further augmented by subsequent ICI therapy is reasonable and was one of the

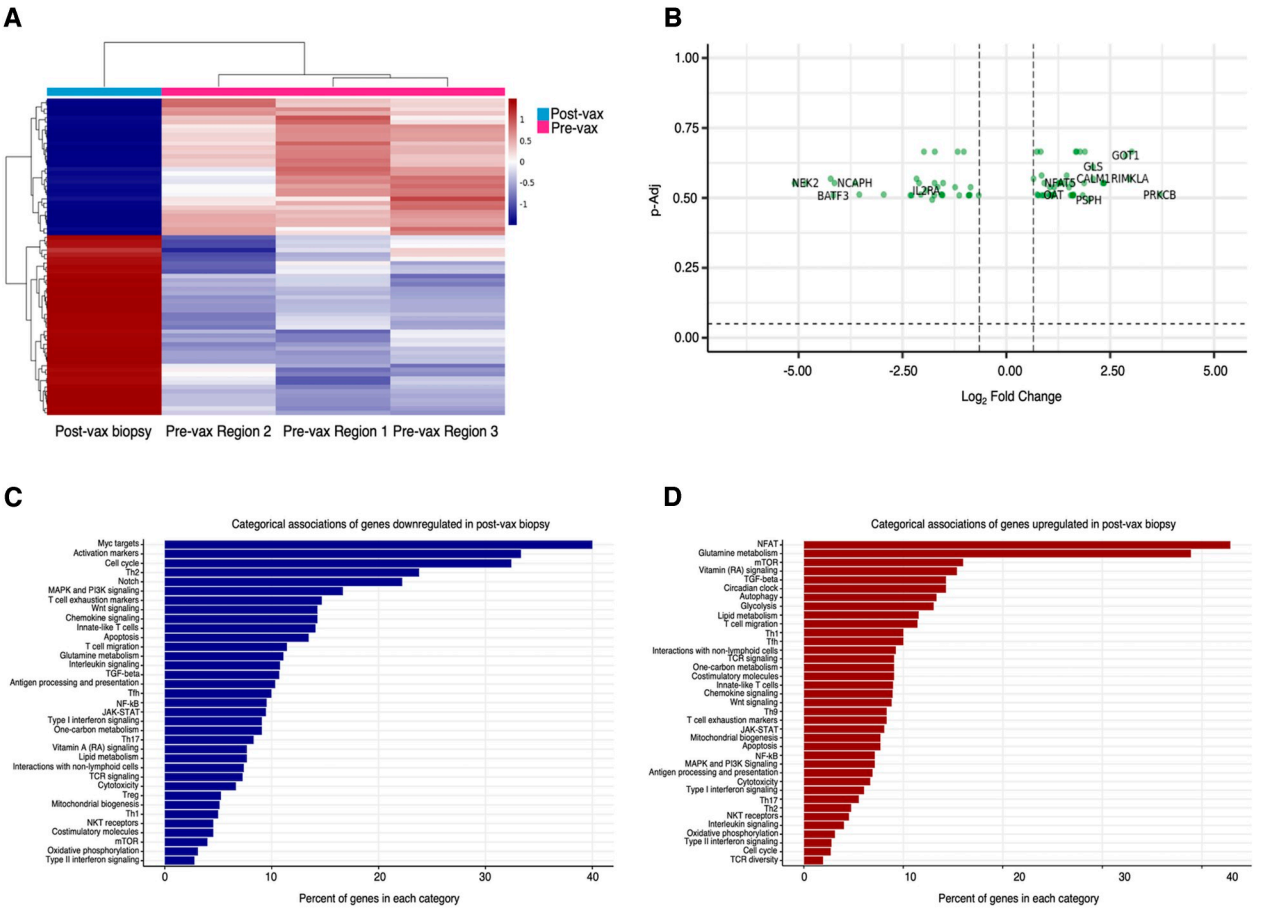

Figure 6.

Differentially expressed genes from the CAR-T Characterization Panel (NanoString) pre- and post-NeoVax in subject 3. **A,** Genes differentially expressed when comparing post-vax biopsy sample with the three pre-vax regions. Seventy-six genes are displayed with a fold change of at least 1.5. **B,** Volcano plot displaying the differentially expressed genes with some of the top fold change genes of interest labeled. **C,** Categorical associations of genes downregulated in the post-NeoVax tumor biopsy. Percent of downregulated genes in each category is displayed. **D,** Categorical associations of genes upregulated in the post-NeoVax tumor biopsy. Percent of upregulated genes in each category is displayed.

main hypotheses to be tested in this study. Unfortunately, the rapid functional decline at time of recurrence of the enrolled subjects confounded the interpretation of the impact of sequential nivolumab postvaccination. Recent studies have demonstrated the possible benefit of anti-PD1 therapy given concurrently with the peptide vaccine (8, 9), which is one strategy that could potentially bypass the concern for rapid functional decline with progression. As such, we are now actively evaluating the concurrent administration of a personalized neoantigen vaccine with PD1 blockade therapy in a separate study (NCT05743595) in newly diagnosed patients with GBM.

Collectively, the data reported here raise several interesting points for consideration that will need to be explored in future iterations of these vaccine trials. The incorporation of multisector sampling increased the neoantigen pool by an average of 40% across all four subjects (range 21.5%–57.5%) when comparing the tumor region with the least number of variants to the number of variants identified from sampling all regions (Supplementary Fig. S9). Due to the limited number of neoantigens that could be successfully included in the peptide vaccine approach because of cost and manufacturing constraints, we prioritized inclusion of shared neoantigens in order to maximize the potential to target the majority of tumor cells (24). However, subsequent studies using a vaccine platform that can accommodate a higher neoantigen payload to allow the targeting of these additional private neoantigens are needed to prospectively test their immunogenicity and impact on vaccine efficacy. Similarly, although targeting 20 neoantigens for vaccine development may be sufficient for most subjects, two of the four subjects described in this study had more than 20 neoantigens that met the criteria for inclusion in the vaccine. We used stringent criteria to rank order our candidate neoantigens; however, we know that RNA expression does not always reflect protein expression, and HLA binding prediction algorithms are imperfect especially for rarer HLA alleles. Moreover, using an IC_{50} threshold of less than 500 nM is largely arbitrary. Thus, a vaccine platform allowing a larger payload to target more neoantigens (on the order of 40–50) would also allow for broader inclusion of shared and private neoantigens without arbitrary filtering and provide an unbiased approach to screen for immunogenicity.

The low production rate of neoantigen-derived SLP is concerning as it may impact the efficacy of the vaccine because a highly targetable neoantigen could be excluded simply due to lack of successful synthesis. Moreover, any neoantigen SLP that cannot be manufactured is not able to be evaluated for immunogenicity which is critical for the improvement of *in silico* prediction algorithms and neoantigen selection criteria. Although many of the failed SLPs likely could be resynthesized with modifications to the peptide structure (length, hydrophobicity, and amino acids), this is not clinically feasible in the setting of an aggressive cancer like GBM or economically feasible. Thus, a vaccine approach that can successfully deliver all selected candidate neoantigens, like a nucleic acid vector, may be more desirable (17, 25). We are currently evaluating the efficacy of a personalized neoantigen DNA–based vaccine in a separate study (NCT04015700) for patients with newly diagnosed, unmethylated GBM.

A rate limiting step in this present trial was the turnaround time from vaccine design to administration as it did not meet the prespecified time point for feasibility (4 weeks post-radiation). There are several points along the manufacturing process that can cause delays including sequencing, prediction algorithm computation, manual review of candidates, peptide design, peptide manufacturing, and product release testing. A vaccine pipeline that will allow for design and manufacturing within a time frame suitable to begin immunizations upon completion of radiotherapy is important, especially in a disease type like GBM in which recurrence can occur early. Any delay in vaccine development, even a month or two, may greatly impact the efficacy of the vaccine treatment approach as it can take several months for the subject to reach peak response after initial vaccination, at which point, they may already have developed recurrent disease with an altered neoantigen landscape. Therefore, as with considerations of improved neoantigen payload and deliverability, an expedited vaccine production platform is an imperative factor that needs to be addressed moving forward.

With regard to immunogenicity, each of the three vaccinated subjects demonstrated increased reactivity to respective NeoVax neoantigens postvaccination (**Fig. 4D–M**). In total, reactivity was noted to a combined 10 of 28 NeoVax containing neoantigens for a hit rate of 36%. Although the lack of additional clinical specimens precluded further experiments to deconvolute whether these responses were CD8 and/or CD4 T-cell–specific, these results are consistent with previously reported reactivity following SLP neoantigen vaccine in melanoma and GBM (8, 10–12, 26). Induction of antigen-specific T-cell responses postvaccine was further supported by immunoSEQ analysis demonstrating the emergence of new CDR3 TCRβ sequences in the postvaccination PBMCs. These emergent clones may be associated with the generation of neoantigen-specific T-cell responses as they did not match to any known viral or cancer-associated TCR (**Fig. 4A–C**). Of course, more definitive studies are needed to further support this assertion but, unfortunately, additional resources are not available to conduct the necessary validation studies.

In conclusion, the collective findings from these analyses suggest NeoVax stimulated the expansion of neoantigen-specific effector T cells. The observed effects of NeoVax on the tumor and its immune microenvironment are encouraging and these results will guide the development of next generation neoantigen vaccine–based clinical trials in patients with GBM.

Authors' Disclosures

A.H. Kim reports grants from Stryker and a consultantship with Monteris Medical. No disclosures were reported by the other authors.

Author Contributions

T.M. Johanns: Conceptualization, formal analysis, writing–original draft, supervision, methodology, resources, funding acquisition; **E.A.R. Garfinkle:** Conceptualization, formal analysis, writing–original draft; **K.E. Miller:** Conceptualization, formal analysis, supervision; **A.J. Livingstone:** Investigation, formal analysis; **K.F. Roberts:** Investigation, formal analysis; **L.P. Rao Venkata:** Investigation; **J.L. Dowling:** Investigation, resources; **M.R. Chicoine:** Investigation, resources; **R.G. Dacey:** Investigation, resources; **G.J. Zipfel:** Investigation, resources; **A.H. Kim:** Investigation, resources; **E.R. Mardis:** Conceptualization, supervision; **G.P. Dunn:** Conceptualization, supervision, resources, funding acquisition.

Acknowledgments

K.E. Miller and E.R. Mardis were supported by the Nationwide Foundation Innovation Fund. T.M. Johanns was supported by NIH K12 Award K12CA167540 and The Alvin J. Siteman Cancer Center Investment Program along with The Foundation for Barnes-Jewish Hospital. G.P. Dunn was supported by NIH NINDS R01NS112712 and The Schnuck Family Fund and The Knight and Christopher Davidson Family Fund. We thank the patients for their participation in the research study and physicians and staff at Barnes-Jewish Hospital and the Department of Neurosurgery at Washington University School of Medicine in St. Louis.

Note

Supplementary data for this article are available at Clinical Cancer Research Online (http://clincancerres.aacrjournals.org/).

Received October 16, 2023; revised January 18, 2024; accepted April 15, 2024; published first April 19, 2024.

References

1. Stupp R, Mason WP, van den Bent MJ, Weller M, Fisher B, Taphoorn MJB, et al. Radiotherapy plus concomitant and adjuvant temozolomide for glioblastoma. N Engl J Med 2005;352:987–96.
2. Hegi ME, Diserens AC, Gorlia T, Hamou MF, de Tribolet N, Weller M, et al. MGMT gene silencing and benefit from temozolomide in glioblastoma. N Engl J Med 2005;352:997–1003.
3. Ostrom QT, Cioffi G, Waite K, Kruchko C, Barnholtz-Sloan JS. CBTRUS statistical report: primary brain and other central nervous system tumors diagnosed in the United States in 2014 to 2018. Neuro Oncol 2021;23(12 Suppl 2):iii1-105.
4. Omuro A, Brandes AA, Carpentier AF, Idbaih A, Reardon DA, Cloughesy T, et al. Radiotherapy combined with nivolumab or temozolomide for newly diagnosed glioblastoma with unmethylated MGMT promoter: an international randomized phase III trial. Neuro Oncol 2023;25:123–34.
5. Lim M, Weller M, Idbaih A, Steinbach J, Finocchiaro G, Raval RR, et al. Phase III trial of chemoradiotherapy with temozolomide plus nivolumab or placebo for newly diagnosed glioblastoma with methylated MGMT promoter. Neuro Oncol 2022;24:1935–49.
6. Lassman AB, Pugh SL, Wang TJC, Aldape K, Gan HK, Preusser M, et al. Depatuxizumab mafodotin in EGFR-amplified newly diagnosed glioblastoma: a phase III randomized clinical trial. Neuro Oncol 2023;25:339–50.
7. Rocha Pinheiro SL, Lemos FFB, Marques HS, Silva Luz M, de Oliveira Silva LG, Faria Souza Mendes Dos Santos C, et al. Immunotherapy in glioblastoma treatment: current state and future prospects. World J Clin Oncol 2023;14:138–59.
8. Ott PA, Hu-Lieskovan S, Chmielowski B, Govindan R, Naing A, Bhardwaj N, et al. A phase Ib trial of personalized neoantigen therapy plus anti-PD-1 in patients with advanced melanoma, non-small cell lung cancer, or bladder cancer. Cell 2020;183:347–62.e24.

9. Awad MM, Govindan R, Balogh KN, Spigel DR, Garon EB, Bushway ME, et al. Personalized neoantigen vaccine NEO-PV-01 with chemotherapy and anti-PD-1 as first-line treatment for non-squamous non-small cell lung cancer. Cancer Cell 2022;40:1010–26.e11.
10. Keskin DB, Anandappa AJ, Sun J, Tirosh I, Mathewson ND, Li S, et al. Neoantigen vaccine generates intratumoral T cell responses in phase Ib glioblastoma trial. Nature 2019;565:234–9.
11. Johanns TM, Miller CA, Liu CJ, Perrin RJ, Bender D, Kobayashi DK, et al. Detection of neoantigen-specific T cells following a personalized vaccine in a patient with glioblastoma. Oncoimmunology 2019;8:e1561106.
12. Hilf N, Kuttruff-Coqui S, Frenzel K, Bukur V, Stevanović S, Gouttefangeas C, et al. Actively personalized vaccination trial for newly diagnosed glioblastoma. Nature 2019;565:240–5.
13. Schaettler MO, Richters MM, Wang AZ, Skidmore ZL, Fisk B, Miller KE, et al. Characterization of the genomic and immunologic diversity of malignant brain tumors through multisector analysis. Cancer Discov 2022;12:154–71.
14. Kelly BJ, Fitch JR, Corsmeier DJ, Zhong H, Wetzel AN, et al. Churchill: an ultra-fast, deterministic, highly scalable and balanced parallelization strategy for the discovery of human genetic variation in clinical and population-scale genomics. Genome Biol 2015;16:6.
15. Hundal J, Carreno BM, Petti AA, Linette GP, Griffith OL, Mardis ER, et al. pVAC-Seq: a genome-guided *in silico* approach to identifying tumor neoantigens. Genome Med 2016;8:11.
16. Richters MM, Xia H, Campbell KM, Gillanders WE, Griffith OL, Griffith M. Best practices for bioinformatic characterization of neoantigens for clinical utility. Genome Med 2019;11:56.
17. Rojas LA, Sethna Z, Soares KC, Olcese C, Pang N, Patterson E, et al. Personalized RNA neoantigen vaccines stimulate T cells in pancreatic cancer. Nature 2023;618:144–50.
18. Mahlokozera T, Vellimana AK, Li T, Mao DD, Zohny ZS, Kim DH, et al. Biological and therapeutic implications of multisector sequencing in newly diagnosed glioblastoma. Neuro Oncol 2018;20:472–83.
19. DeWitt WS, Emerson RO, Lindau P, Vignali M, Snyder TM, Desmarais C, et al. Dynamics of the cytotoxic T cell response to a model of acute viral infection. J Virol 2015;89:4517–26.
20. Rytlewski J, Deng S, Xie T, Davis C, Robins H, Yusko E, et al. Model to improve specificity for identification of clinically-relevant expanded T cells in peripheral blood. PLoS One 2019;14:e0213684.
21. Chronister WD, Crinklaw A, Mahajan S, Vita R, Koşaloğlu-Yalçın Z, Yan Z, et al. TCRMatch: predicting T-cell receptor specificity based on sequence similarity to previously characterized receptors. Front Immunol 2021;12:640725.
22. Miller CA, White BS, Dees ND, Griffith M, Welch JS, Griffith OL, et al. SciClone: inferring clonal architecture and tracking the spatial and temporal patterns of tumor evolution. PLoS Comput Biol 2014;10:e1003665.
23. Cloughesy TF, Mochizuki AY, Orpilla JR, Hugo W, Lee AH, Davidson TB, et al. Neoadjuvant anti-PD-1 immunotherapy promotes a survival benefit with intratumoral and systemic immune responses in recurrent glioblastoma. Nat Med 2019;25:477–86.
24. Westcott PMK, Muyas F, Hauck H, Smith OC, Sacks NJ, Ely ZA, et al. Mismatch repair deficiency is not sufficient to elicit tumor immunogenicity. Nat Genet 2023;55:1686–95.
25. Bausart M, Vanvarenberg K, Ucakar B, Lopes A, Vandermeulen G, Malfanti A, et al. Combination of DNA vaccine and immune checkpoint blockades improves the immune response in an orthotopic unresectable glioblastoma model. Pharmaceutics 2022;14:1025.
26. Ott PA, Hu Z, Keskin DB, Shukla SA, Sun J, Bozym DJ, et al. An immunogenic personal neoantigen vaccine for patients with melanoma. Nature 2017;547:217–21.